Applied Ocean Research 129 (2022) 103403

Contents lists available at ScienceDirect

Applied Ocean Research

journal homepage: www.elsevier.com/locate/apor

International benchmark study on numerical simulation of flooding and motions of a damaged cruise ship

Pekka Ruponen [a,b,*], Rinnert van Basten Batenburg [c], Riaan van't Veer [c], Luca Braidotti [d], Shuxia Bu [e], Hendrik Dankowski [f], Gyeong Joong Lee [g], Francesco Mauro [h,i], Eivind Ruth [j], Markus Tompuri [a]

[a] NAPA, Finland
[b] Department of Mechanical Engineering, Marine Technology, Aalto University, Finland
[c] MARIN, the Netherlands
[d] University of Trieste, Italy
[e] CSSRC, China
[f] University of Applied Science Kiel, Germany
[g] KRISO, Republic of Korea
[h] MSRC, University of Strathclyde, UK
[i] Department of Maritime and Transport Technology, Faculty of Mechanical, Maritime and Materials Engineering, Delft University of Technology, the Netherlands
[j] DNV, Norway

ARTICLE INFO

Keywords:
Damaged ship stability
Progressive flooding
Transient flooding
Validation
Physical tests
Numerical methods
International benchmark

ABSTRACT

Large cruise ships can carry 10 000 persons onboard, and consequently, survivability of the ship in the event of a flooding accident is essential. Many designers are already conducting advanced damage stability analyses beyond the regulatory requirements. With increased computing capacity, survivability analyses, by using time-domain simulation tools, are already commonly applied in the design of new cruise ships. Consequently, it is essential that such tools are properly validated, in terms of ship response and detailed flooding behavior, to assess the capability and applicability of the tools. For this purpose, an international benchmark study on simulation of flooding and motions of damaged cruise ships was conducted within the EU Horizon 2020 project FLARE, using experimental data from new dedicated model tests as a reference. The test cases include transient and progressive flooding, both in calm water and in irregular beam seas. The results indicate that capsize is properly captured by simulation codes, but there are notable differences in the flooding progression and capsize mechanisms, especially when flooding takes place in high waves.

1. Introduction

Flooding of a damaged ship is a very complex process, and consequently, accurate numerical modelling of the relevant fluid structure interactions is challenging. During the past two decades, there has been significant development in numerical tools for simulation of the flooding process and motions of damaged ships. An overview of these advancements was presented by Papanikolaou (2007). The subsequent progress is discussed e.g. in the review papers by Bačkalov et al. (2016) and Manderbacka et al. (2019). Such simulations have been used for various studies on damage survivability of passenger ships, as presented in e.g. van't Veer et al. (2004), Spanos and Papanikolaou (2014), Vassalos (2016), Ruponen et al. (2019), Atzampos et al. (2019), Braidotti et al. (2021) and Mauro et al. (2022). With increasing importance of survivability studies in the design of passenger ships, a thorough validation and benchmarking of the simulation methods is considered essential.

The applied simulation tools are usually based on hydraulic model with Bernoulli's theorem. However, recently the use of computational fluid dynamics (CFD) tools for simulation of the flooding process has expanded from the simple scenarios, Gao et al. (2010) and cross-flooding analyses, Ruponen et al. (2012), to extensive simulations of flooding and motions of a damaged ship in waves, Caldas et al. (2018) and Ruth et al. (2019). Consequently, comparison of different types of simulation tools is also relevant.

* Corresponding author at: Department of Mechanical Engineering, Marine Technology, Aalto University, NAPA, PO Box 470, FI-00181 Helsinki, Finland.
E-mail address: pekka.ruponen@napa.fi (P. Ruponen).

https://doi.org/10.1016/j.apor.2022.103403
Received 26 July 2022; Received in revised form 30 September 2022; Accepted 31 October 2022

Over the years, flooding and damage stability of ships have been studied experimentally with scale models. Especially, after the rapid capsize and sinking of the passenger/ro-ro (ropax) vessel Estonia in 1994, so-called Stockholm Agreement model tests were performed, both for existing ships and new designs, Schindler (2000). Later also more complex arrangements of flooded compartments have been studied. Ikeda et al. (2003) conducted flooding tests with a small model (1:185) of a large cruise ship, and later with a larger scale (1:50) section of the same ship, Ikeda et al. (2011), focusing on the effects of the internal layout of the flooded compartments. Within the SAFENVSHIP (2002–2006) project, transient and progressive flooding of a large cruise ship were studied experimentally, and the main results were reported by Italy (2004a, 2004b) at IMO SLF47 meeting. In addition, Cho et al. (2009) have presented flooding tests for a cruise ship model with simplified compartment arrangement. However, experimental data on cruise ship flooding was not available for validation of benchmarking purposes.

Progressive flooding has also been studied experimentally with simplified hull geometries, Ruponen et al. (2007) and Lorkowski et al. (2014). The former being used also in a benchmark study by ITTC (International Towing Tank Conference), and widely as a validation material for various numerical codes. In addition, navy vessels with complex internal arrangement in the flooded compartments have been studied in model scale by Macfarlane et al. (2010) and in full ship scale by Ruponen et al. (2010).

During the past two decades, several benchmark studies on damaged ship stability and motions in waves have been organized, mainly within the ITTC. In the first study, Papanikolaou and Spanos (2001), the roll motion and the limiting significant wave height were studied for a passenger/ro-ro ferry with one damage case, involving also the main vehicle deck. The focus was solely on the seakeeping characteristics of a flooded ship in waves. The next ITTC benchmark, described by Papanikolaou and Spanos (2005), was more extensive, including also transient flooding process of a ro-ro/passenger ship in calm water, based on experimental results from the EU FP5 project HARDER (2000–2003), reported by van't Veer (2001).

The third ITTC benchmark study focused on progressive flooding in a large-scale (about 1:10) box-shaped barge model, Ruponen et al. (2007). The results are reported by van Walree and Papanikolaou (2007). Motions of the barge were fully quasi-static, and discharge coefficients for all openings were shared in advance, but still the results showed large variation in the progressive flooding.

A further benchmark study on transient flooding and capsize of a ro-ro/passenger ship in waves, with model test results from van't Veer (2001), was carried out within the EU FP6 project SAFEDOR (2005–2009) and summarized by Papanikolaou and Spanos (2008). The significant wave height at the survival boundary was estimated quite well by two out of the four participants. However, it was also concluded that the detailed background analysis showed that codes simulated the test phenomena in a substantially different way.

The recommendations of the previous benchmark studies clearly indicate a need for further studies, focusing on the different phenomena and fluid structure interactions involved in the flooding process of ships with complex internal arrangement. Moreover, new flooding simulation tools have been developed, further emphasizing the need for a new international benchmark study.

Although several experiments have been done with various ship models, there is not enough publicly available test data for proper benchmarking of numerical methods. Consequently, dedicated model tests were conducted within the EU Horizon 2020 project, FLARE (2018–2022), focusing on progressive flooding in a typical large cruise ship with complex arrangement of flooded compartments, both in calm water and in beam seas.

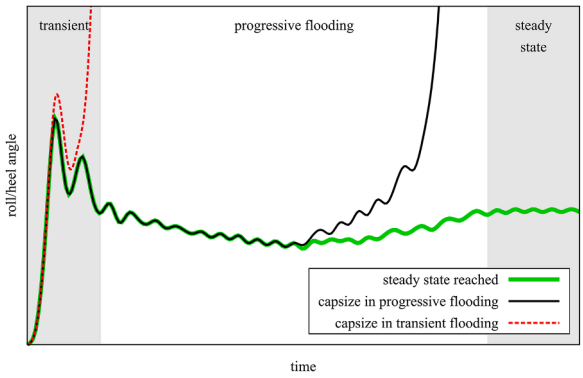

Fig. 1. Schematic visualization of the different stages of flooding process.

2. Objectives

The flooding process can be divided into three separate stages with distinctive characteristics. The transient flooding stage involves rapid inflow to the damaged compartments, typically resulting in a large roll angle, or even rapid capsize. This stage may be followed by progressive flooding to undamaged compartments through various internal openings. This stage can last for a very long time for ships with dense non-watertight internal subdivision. The progressive flooding can be so extensive that the ship capsizes. If the ship does not sink or capsize during this stage, a final steady state is reached. These different flooding stages are visualized in Fig. 1.

The previous benchmark studies have mainly focused on the stability and motions of a damaged ship in the steady state condition after flooding. In addition, both transient flooding and progressive flooding stages have been studied in simplified scenarios. Furthermore, the previous part of the FLARE benchmark study focused on flooding and capsizing of a ropax ship, without any internal non-watertight subdivision in the flooded compartments, as presented in Ruponen et al. (2022). Since the capsize mechanisms can be notably different for ropax and cruise ships, another benchmark study was considered necessary, since flooding scenarios with actual capsize either during the transient or progressive flooding stage had not yet been studied experimentally for a ship model with complex arrangement of flooded compartments. Within the EU Horizon 2020 project FLARE, such model tests were conducted at MARIN, and the results are used as a reference data for a new international benchmark study.

3. Benchmark setup

3.1. Methodology

The flooding process is strongly coupled with the motions of the damaged ship. Flooding process affects damaged ship motions, and vice versa. In addition, the presence of waves has an impact on both the flooding process and the ship motions, as visualized in Fig. 2. Previously, Ypma and Turner (2019) have presented a new approach for validation of flooding simulation, considering both captive and freely floating model tests. In the FLARE benchmark study, the flooding part was first studied with captive model tests in calm water, Ruponen et al. (2021). Transient and gradual flooding of a damaged ropax vessel, with two open damaged compartments and large vehicle deck were studied separately, Ruponen et al. (2022). For a ship with dense internal subdivision in the watertight compartments the flooding and capsize mechanisms are known to be different from ropax vessels, and therefore, in this follow-up study with a model of a typical large cruise ship, flooding in calm water and in irregular beam seas are investigated.

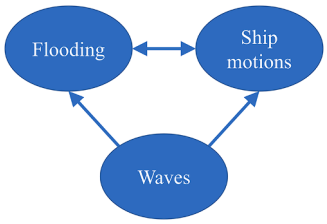

Fig. 2. Visualization of the couplings between waves, flooding and ship motions.

3.2. Cruise ship model[1]

An unbuilt large cruise ship design (about 95 900 GT) was provided by Chantiers de l'Atlantique. Tests were carried out at MARIN with a model built in scale 1:60, Fig. 3. A model of the studied ship was constructed in scale 1:60. The bow and stern are filled with Styrofoam, and the floodable compartments are made from transparent PVC. The sections were stiffened by two carbon fiber box beams on top of the model.

The main dimensions are listed in Table 1 and the hull form is shown in Fig. 4. The hull of the model extends vertically over 8 decks, and floodable rooms are located on 6 lower decks, as shown in Fig. 5. In total, the model contains 60 floodable rooms bounded by bulkheads and decks. The rooms are connected by 82 internal openings in the bulkheads and 11 openings in the decks. The actual geometry of the model was distributed, and each participant modelled the arrangement based on their own practices and expertise. Thickness of the plexiglass decks and bulkheads is 4 mm (in model scale), and it was recommended to model actual compartment limits accurately and apply a permeability of 1.0 for each room, instead of simply adjusting the permeability to account for the volume occupied by the decks and bulkheads. The bulkhead deck arrangement (Deck 4 in Fig. 5) is the same that was studied in the deck flooding in captive model test for the first part of the FLARE benchmark study, Ruponen et al. (2021).

The deepest subdivision draft of 8.20 m was selected for the test condition. According to current SOLAS Ch. II-1 requirements the smallest allowed metacentric height (GM) at this draft is 3.50 m. Based on initial simulation and model test results, notably smaller GM was needed to achieve also capsize cases in a sea state with a significant wave height of 4.0 m. Consequently, a GM value of 2.36 m was selected for the benchmark cases.

The studied large 3-compartment damage scenario was selected by MSRC, based on initial simulations for the original ship design and subdivision with PROTEUS software, using standard discharge coefficient 0.6 and assuming thin decks and bulkheads. Further simplifications were done in the construction of the model, and consequently, the actual damage scenario differs from the one used in the initial simulations.

The breach is on the starboard side, forward from amidships. Vertically the breach extends over 6 decks from the baseline. The flooding case is asymmetric, and the modelled geometry is a simplification of the original design, provided by Chantiers d'Atlantique.

3.3. Scope and structure

The benchmark study focuses on both flooding progression and motions of a damaged cruise ship, and contains three separate test cases:

(1) Transient flooding in calm water.
(2) Transient and progressive flooding in irregular beam seas.
(3) Up-flooding in calm water with smaller breach size.

[1] Detailed geometry and drawings of the model are available on request from the corresponding author

The benchmark was open to participants outside the FLARE consortium, and various organizations with recently published studies on flooding simulation were invited beforehand. Eventually eight organizations provided numerical results to the benchmark study. A summary of the participation in the benchmark study is presented in Table 2. The relevant experimental data (time histories of key quantities, such as roll angle, and videos of the tests) were shared beforehand to all participants in order to enable fair and equal benchmarking conditions.

In general, the codes can be categorized based on the treatment of floodwater:

- simplified model with the free surfaces in flooded rooms modelled as horizontal planes,
- inclined plane, based on an apparent gravity (lumped mass) or a simplified dynamic resonance model,

- Volume of Fluid (VOF) type of Computational Fluid Dynamics (CFD) model with compartments discretized into a mesh of computational cells.

The category of each code is also listed in Table 2.

The applied codes are mainly in-house software, developed and maintained at a university or a research institution. The exceptions are NAPA and Star-CCM+ (used by DNV), which are commercially available. Furthermore, the code PROTEUS, used by MSRC, is currently managed by Safety at Sea Ltd.

3.4. Overview of the numerical simulation methods

3.4.1. CSSRC

In-house code **wDamstab**. Bernoulli's equation is used for calculation of flooding rates through openings and horizontal flat plane is assumed for floodwater surfaces. Four degrees of freedom (sway, heave, roll and pitch) are considered. Ship motion is calculated based on the potential flow theory, namely Salvesen–Tuck–Faltinsen (STF) strip theory. Froude-Krylov and hydrostatic forces are calculated based on the integration of pressure over the instantaneous wet surface. More details are given in Bu et al. (2018), (2020), in Chinese.

3.4.2. DNV

CFD results for the Case 3 with **Star-CCM+** software. A mesh of about 3 million cells, using an overset mesh approach with a time step of 0.002 s was used. Model scale was used, and the results have been converted to full scale for comparison with the other codes. Also the ventilation pipes were modelled and calculations included the air flows. The model was free in all 6 degrees of freedom. The simulation was conducted with laminar flow and without prism layers to reduce computation time. Laminar flow was considered a reasonable assumption since the simulation was performed in model scale. Including prism layers would have improved the modeling of the water-wall friction, but this was believed to be of minor importance compared to the flooding dynamics.

3.4.3. KRISO

In-house code **SMTP** was used with flooding rates calculated by Bernoulli's equation and empirical discharge coefficients. The floodwater in compartments can be modeled either with a horizontal free surface or with a dynamic model in which the equation of motion of the mass center is solved using the tank resonance mode of the standing wave for the instantaneous water depth, and the resulting inclined free surface is used for the calculation of the pressure at openings. The compartments are treated independently, so the model can be selected appropriately to represent the property of each compartment. Ship motions are calculated by 6-DOF non-linear equations in time-domain, in which the Froude-Krylov and restoring forces are calculated for instantaneous wetted surface, and the hydrodynamic forces are

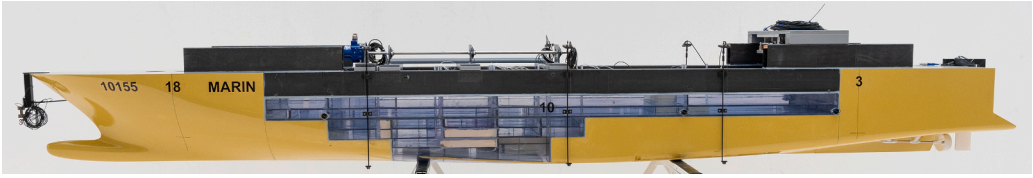

Fig. 3. Model of the cruise ship, courtesy of MARIN.

Table 1
Main dimensions of the studied cruise ship and the applied initial intact condition in model tests.

	Full scale	Model scale
Length over all	About 300 m	About 5.0 m
Length between perpendiculars	270.00 m	4.5 m
Breadth	35.20 m	0.587 m
Draught (in tests)	8.20 m	0.137 m
Trim (in tests)	0.00 m	0.000 m
Height of bulkhead deck form base line	11.00 m	0.183 m
Gross tonnage	95 900	-
Metacentric height (in tests)	2.36 m	0.0393 m
Radius of inertia for roll	13.904 m	0.2317 m

calculated by the traditional strip method. The floodwater affects the ship motion as internal forces, not as external forces. In other words, it changes the mass and its center of gravity resulting in changes of the inertial and gravity forces. Details are presented in Lee (2015a), (2015b). For this study, the dynamic resonance model was selected for the compartments with a connection to the sea. The air flows were calculated for all compartments and the air pipes were modeled as in model test pictures.

3.4.4. MARIN

The Extensible Modelling Framework (**XMF**) is a software toolkit on which all MARIN's fast-time and real-time simulation software is based applying Newtonian dynamics, of which Fredyn and ANySim are known examples. XMF is recently extended with a flooding module library (XHL) based on Bernoulli's equation with empirical discharge coefficients, using generic 3D defined floodable objects. A graph-solver technique is utilized to capture the complexity of entrapped air in compartments and for hydrostatic pressure-corrections from fully flooded compartments. To account for the flow inertia effects in the progression of flood water through the ship, the XMF framework is recently extended with a new inertia-based flow solver, denoted as the unified internal flow (UIF) module. The theory and first results of this solver are presented in van't Veer et al. (2021). The ship hydrodynamics were calculated by program SEACAL using zero-speed Green functions. The complete underwater part of the hull was represented by 14544 flat quadrilateral panels in the potential flow calculations. During the simulations the complete 3D ship hull is used. Retardation functions were constructed for the upright hull at initial draft and used to represent the hull radiation forces in time domain. The diffraction loads are calculated through the pre-computed RAO functions. The incident wave pressures are integrated on the actual submerged hull volume under the incident wave profile. In each flooded compartment the water surface is a flat plane with a normal vector pointing perpendicular to the resulting effective gravity angle(s) composed from all 6-DOF rigid body accelerations. To obtain this, the local gravity angle is calculated in each last known center of mass in each compartment. The center of mass is calculated based on the 3D object geometry, water surface orientation and actual volume of water in the compartment. The horizontal mooring system was modeled, and full ventilation was assumed in all simulations.

3.4.5. MSRC

In-house code **PROTEUS** owned by Safety at Sea Ltd., and originally developed at University of Strathclyde (MSRC). Flooding rates are calculated applying Bernoulli's equation with a hard-coded discharge coefficient of 0.6. The code has a feature for Free-Mass-In-Potential-Surface (FMPS), Papanikolaou et al. (2000), where the whole mass of water in the compartment is treated as a single point mass. However, in this benchmark study, the current default setting, where the FMPS model is omitted, was used. Consequently, the calculation assumes that the water level inside a compartment is always parallel to the

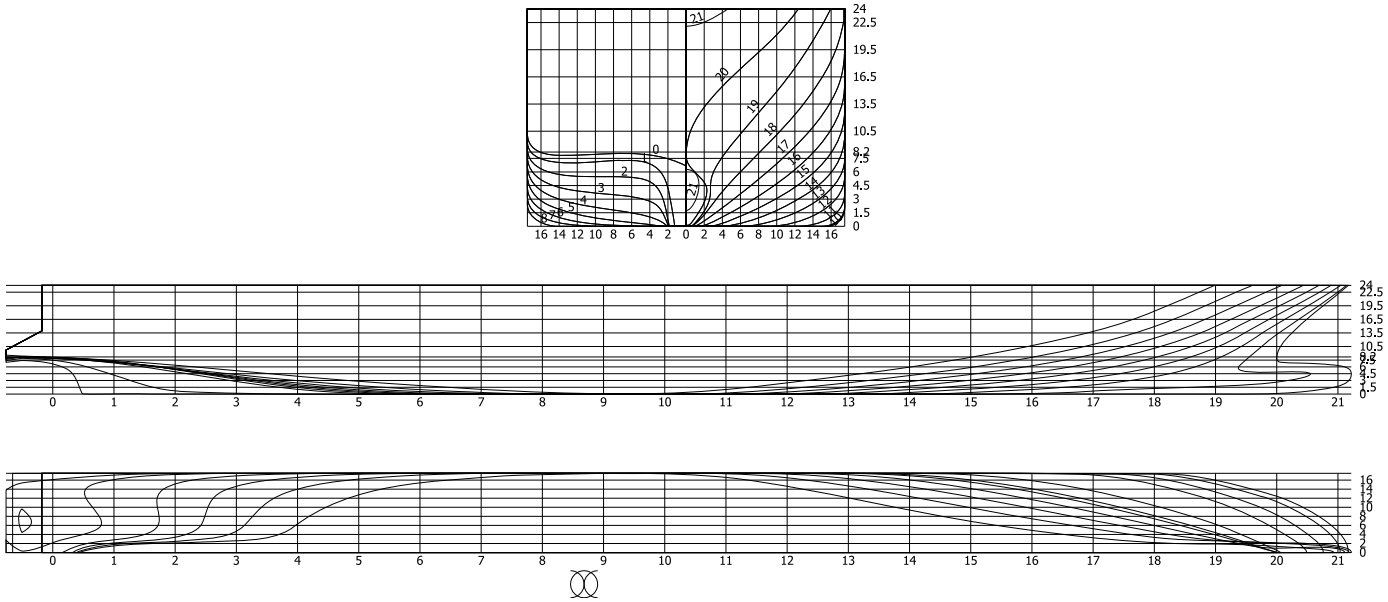

Fig. 4. Lines drawing of the bare hull of the studied cruise ship.

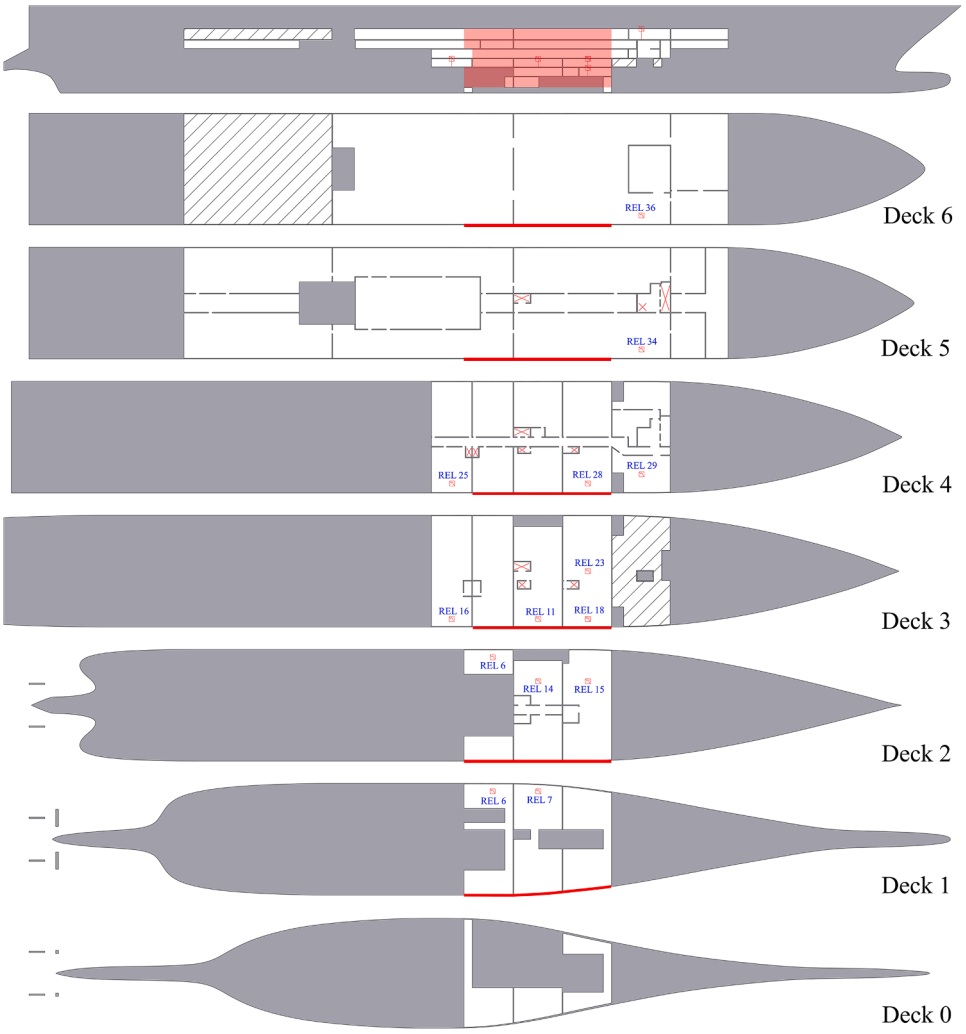

Fig. 5. Arrangement of the ship model; the hatched rooms were filled with foam and thus not floodable, and the red squares mark the selected water level sensors, red × symbols denote holes in the deck and thick red lines mark the large breach.

Table 2
Summary of the participation in the benchmark study (symbol ✓ denotes participation in the case).

ID	Participant	Code	Treatment of floodwater surface	Case 1: large breach in calm water	Case 2: large breach in waves	Case 3: small breach in calm water
CSSRC	China Ship Scientific Research Center (CHI)	wDamstab	Horizontal plane	✓	✓	✓
DNV	DNV (NOR)	Star-CCM+	VOF	–	–	✓
KRISO	Korea Research Institute of Ships & Ocean Engineering (ROK)	SMTP	Inclined plane	✓	✓	✓
MARIN	Maritime Research Institute Netherlands (NED)	XMF	Inclined plane	✓	✓	✓
MSRC	Maritime Safety Research Center (UK)	PROTEUS	Horizontal plane	✓	✓	✓
NAPA	NAPA (FIN)	NAPA	Horizontal plane	✓	✓	✓
UAK	University of Applied Science Kiel (GER)	E4 Flooding	Horizontal plane	✓	–	✓
UNITS	University of Trieste (ITA)	LDAE	Horizontal plane	✓	–	✓

undisturbed sea water level. Froude-Krylov and restoring forces are integrated up to the instantaneous wave elevation both for regular and irregular waves. Radiation and diffraction are derived from 2D strip theory. Hydrodynamic coefficients vary with the attitude of the ship during the flooding process (heave, heel and trim). Details are presented in Jasionowski (2001). In the test cases, motions were evaluated by solving a 4 DOF system of equation (yaw and surge not modelled) assuming the vessel is allowed to drift freely. Hydrodynamic forces for the actual attitude of the vessel are obtained through interpolation on a precalculated set of forces obtained by 2D strip theory calculations. Drift forces are modelled according to empirical formulations, as presented in Letizia (1996).

3.4.6. NAPA

The commercial software **NAPA** is used. The flow rates are calculated from Bernoulli's equation, with user-defined discharge coefficients for each opening. Horizontal flat free surface is assumed in all flooded rooms. Pressure-correction algorithm is applied to solve the governing

equations (continuity and Bernoulli). In the presented simulations, dynamic roll motion was calculated, while draft and pitch were considered quasi-static. The effect of waves on flooding rates was considered. Details are presented in Ruponen (2007), (2014).

3.4.7. UAK

In-house code **E4 Flooding** with flooding calculated by using Bernoulli's equation with horizontal surface and flooding path modelled as directed graphs. In the studied cases, 6-DOF dynamic ship motions were calculated. Linear roll damping was assumed. The code supports simulation either in calm water or in regular waves, and thus results for the Case 2 were not provided. Details are presented in Dankowski (2013) and Dankowski and Krüger (2015).

3.4.8. UNITS

In-house code **LDAE**, developed for fast onboard simulation of progressive flooding, was used. The flooding process is modelled using a DAE (Differential Algebraic Equations) system, based on the Bernoulli equation, which is linearized and solved analytically. A flat horizontal free surface is assumed for the sea and waterplanes inside flooded rooms, while the floating position of the ship is updated at each integration step accounting for floodwater weight. An adaptive integration time step, based on floodwater level derivatives, is adopted. The model does not include dynamic ship motions. Only quasi-steady change of heel, trim and sinkage is considered. A detailed description of the method can be found in Braidotti and Mauro (2019, 2020) and Braidotti et al. (2022).

3.5. Numerical modelling of the compartments

In order to capture the transient asymmetry of flooding with hydraulic simulation models, most participants divided some larger rooms with open connections, following the principle introduced by Santos et al. (2002). The double bottom compartments are wide, and without such numerical subdivision the Bernoulli-based codes are unable to model the transient asymmetric flooding of these compartments, Santos et al. (2002). Each participants modelled the compartments based on their experience and requirements of the applied software. Modelled rooms and connections for the double bottom compartments are visualized in Fig. 6. UAK did not divide the rooms in order to avoid rapid capsize in the transient flooding case. For CFD simulation, the compartments were discretized into computational cells, based on the expertise of the participant, and convergence studies to ensure that the applied grid was fine enough for the purpose.

4. Model tests

4.1. Test arrangement

A magnetic cover sheet closed the breach before the test, Fig. 7. At the start of the flooding (zero time), the coversheet was pulled upwards with a winch. The speed was about 2.5 m/s in model scale. Therefore, the breach was opened very rapidly, in less than 4 s in full scale, and an instant opening time for the breach was applied in the numerical simulations. For practical reasons a nominal capsize limit of 40° was used in the tests. All results are presented in full scale, with roll angle positive to the breach side (starboard) and pitch (trim) angle towards bow is positive. Measurements included 6 DOF motion of the model, as well as water levels in several locations in the flooded compartments.

The floodable compartments were vented with large air pipes on the leeward (intact) side, as visualized in Fig. 8. In this respect, the effects of air compression were considered small, and consequently full ventilation was assumed by most participants. Air pressures inside the model were not measured, so this assumption cannot be confirmed. However,

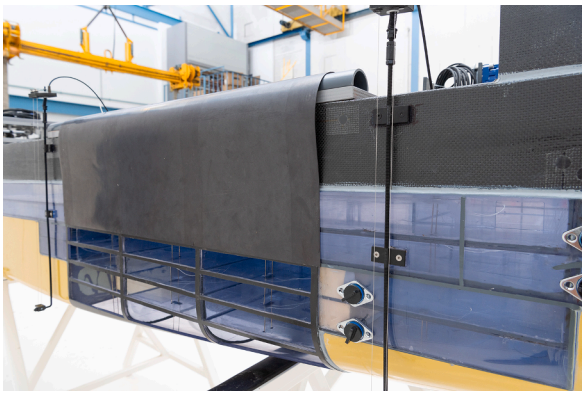

Fig. 7. Breach opening and the magnetic cover (photo courtesy of MARIN).

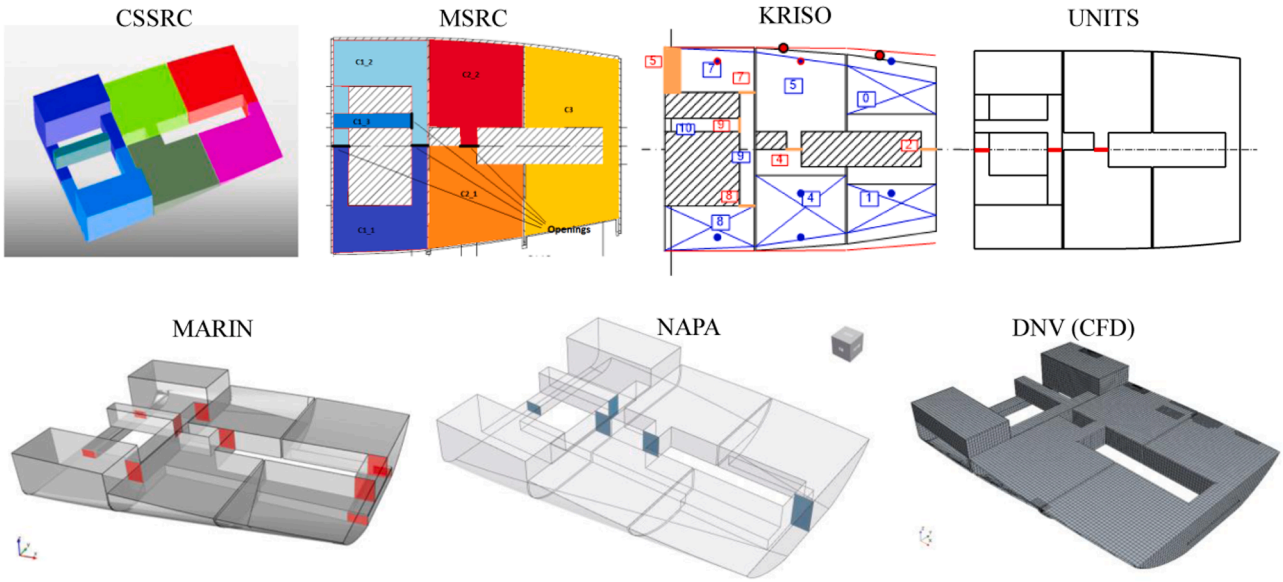

Fig. 6. Modelling of the flooded compartments in the double bottom; for Bernoulli based simulation codes also the openings connecting the parts of the large void spaces are shown.

in the CFD simulations by DNV in model scale, also the air pipes were modelled and formation of small air pockets in some compartments were observed. Also these results indicate that full ventilation is a reasonable assumption in this case.

4.2. Discharge coefficients

Many simulation codes use a hydraulic model, based on Bernoulli's theorem, for calculation of the flow rates through the openings. This approach is efficient, when compared to CFD tools, but it requires semi-empirical discharge coefficients to model the flow losses in the openings. For full scale simulations, the so-called industry standard value $C_d = 0.6$ has proven to be reasonably accurate, see e.g. Ruponen et al. (2010). Since frictional losses are proportional to the Reynolds number, somewhat larger discharge coefficient is characteristic for model-scale openings, Idel'chik (1960). This has also been observed in some recent experimental studies, e.g. Katayama and Ikeda (2005) and Ruponen et al. (2007). Consequently, all participants using Bernoulli's theorem, were recommended to use discharge coefficients given in Table 3. The values were obtained from dedicated experiments carried out at MARIN. The software PROTEUS, used by MSRC, has hard coded discharge coefficient 0.6, and therefore, it was necessary to compensate this by adjusting the opening areas in order to achieve the same effect.

4.3. Hydrostatics

The hull form and arrangement of the floodable compartments were shared to participants in the form of drawings, 3D geometry files and tables. Most participants applied the provided 3D hull form and only KRISO used lofting table data. In order to ensure that the geometry was modelled sufficiently accurately, the volumes of the buoyant hull (up to 20.4 m above the baseline) and displacement (V_{hull} and V_{disp}), as well as the center of the buoyant hull (X_{hull}, Y_{hull}, Z_{hull}) and the center of displacement at intact draft (X_{disp}, Y_{disp}, Z_{disp}) were compared. In addition, the total volume and center of the floodable compartments (V_{rooms}, X_{rooms}, Y_{rooms} and Z_{rooms}) were checked. Results are listed in Table 4, showing good consistency.

The intact metacentric height GM = 2.36 m was obtained from an inclining test of the model, assuming a straight righting lever curve between upright and the achieved inclination of 2.44°. Due to the hull form, the waterplane area changes significantly even at small heel angles. Consequently, the intact stability is sensitive to how accurately the hull geometry is described in the various simulation tools. For the benchmark study the GM was given, and it was up to the participants to define the associated vertical center of gravity (KG) for their simulations. The applied values are listed in Table 5, showing an average KG of 17.51 m, with a standard deviation of 0.089 m and a difference of 0.278 m between the largest and smallest values. Some participants finetuned the KG value to obtain the same final flooding angle as in the model tests, under the assumption that the floodwater distribution in the simulations was equal to that in the model tests.

The discretization and integration methods in the numerical codes are possible sources for inaccuracies, especially related to calculation of the waterplane area surface inertia moment. Moreover, some small variation was also observed in the vertical center of displacement, which is directly affecting the initial stability. Consequently, the static righting lever (GZ) curve of the intact ship, especially at small heel angles, is considered as a more reliable check for correct modelling of the initial condition before flooding. The GZ curves, and corresponding trim angles, with different codes are presented in Fig. 9. At small heel angles the differences are minimal, but most notably the maximum righting lever values are quite different, and this is expected to have some effect on the simulation results at roll angles larger than 20°.

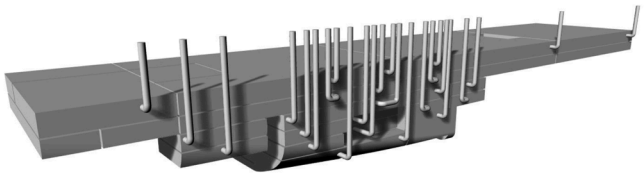

Fig. 8. Rendering of the 3D model of the compartments and ventilation pipes (courtesy of MARIN).

Table 3
Recommended discharge coefficients for the openings.

Opening	C_d	Explanation
Narrow openings (width < 30 mm)	0.73	Based on test at MARIN with opening size 17 mm × 34 mm
Wide openings (width ≥ 30 mm)	0.70	Based on test at MARIN with opening size 47 mm × 34 mm
Breach openings	0.65	Based on test result for 80 mm × 80 mm opening

4.4. Roll decay

The model included simplified propeller and shaft arrangement, as well as rudders and bilge keels. Participants were provided with detailed geometry of the appendages. Furthermore, a roll decay test was performed by MARIN for an intact model, including all appendages. The measured history of roll angle was provided to all participants to help in modelling roll damping characteristics since the focus of the benchmark was on the flooding model performance. The effect of roll damping is notable during the transient flooding stage, but it is not expected to play a major effect in the progressive flooding stage. A comparison of simulated roll decay tests and measurement is shown in Fig. 10. The damping of the roll motion is rather well captured by all codes, but there are still some notable differences. Also the roll period is slightly longer in the simulation by MSRC. The code SMTP, used by KRISO, does not use roll damping input, and instead damping due to wave making is calculated by potential theory and skin friction and eddy making damping are calculated by empirical formulae, including also the appendages.

5. Transient flooding in calm water (Case 1)

In the first benchmark case, transient flooding in calm water is studied. The large breach is opened rapidly, causing a large transient roll angle towards the damage. This is rapidly equalized by cross-flooding on the lower decks in the damaged compartments, and the ship reaches a steady equilibrium since flooding is limited to the breached compartments and the partial bulkheads on the Deck 4 prevent progressive flooding.

The key quantities for comparison are the maximum roll angle and the time-to-flood (TTF). The measured and simulated development of roll and pitch angles are presented in Fig. 11. The maximum measured transient roll angle is 30.7°, and it was reached at about 17.4 s (full scale) after the breach was initiated. After about 90 s, a steady heel angle of 6.7° is achieved.

There is some variation in the maximum simulated transient roll angle, but in general this is slightly underestimated. The smaller second peak in roll motion is qualitatively captured by KRISO and MARIN, i.e. the codes where the water levels in the compartments are considered as inclined planes (Table 2). Also MSRC simulation results in similar roll characteristics, related to transient flooding, although the second peak is very small.

There is also some variation in the final steady state heel angle between the simulation codes, however, the maximum difference to the measured value is only about 0.5°. Both CSSRC and MSRC predict the final steady heel angle very accurately, Fig. 12. UNITS underestimates the final heel, while the other codes overestimate it. However, in general the differences are less than 1°. Small differences in the applied KG (see

Table 4
Comparison of hydrostatics and modelling of compartments (values in full scale).

ID	Buoyant hull (up to 20.4 m from BL)				Displacement at 8.2 m draft				Floodable compartments			
	V_{hull} m^3	X_{hull} m	Y_{hull} m	Z_{hull} m	V_{disp} m^3	X_{disp} m	Y_{disp} m	Z_{disp} m	V_{rooms} m^3	X_{rooms} m	Y_{rooms} m	Z_{rooms} m
CSSRC	161555	126.111	0.000	11.287	51218	127.926	0.000	4.612	47947	149.695	-0.167	13.451
KRISO	161831	126.379	0.000	11.267	51356	127.920	0.000	4.591	48059	149.726	-0.169	13.434
MARIN	164300	124.346	0.000	11.337	51476	127.943	0.000	4.591	47689	149.675	-0.126	13.511
MSRC	162007	126.226	0.000	11.263	51548	127.801	0.000	4.591	48110	149.800	-0.172	13.418
NAPA	162174	126.088	0.000	11.262	51632	127.601	0.000	4.589	48005	149.641	-0.172	13.437
UAK	162063	126.197	0.000	11.262	51608	127.668	0.000	4.591	48005	149.733	-0.177	13.431
UNITS	162003	126.166	0.000	11.272	51477	127.813	0.000	4.596	47993	149.703	-0.171	13.443

Table 5
Applied values of vertical center of gravity KG.

ID	KG (m)
CSSRC	17.580
DNV	17.646
KRISO	17.500
MARIN	17.470
MSRC	17.500
NAPA	17.450
UAK	17.368
UNITS	17.590

Table 5) and possible inaccuracies in the modelling of the flooded compartments and buoyant hull are identified as potential explanations for the observed differences in the final heel angle.

All codes result in slightly larger pitch angle than measured, with UNITS having the best match. The maximum difference is about 0.15°, which is a rather small angle, but still has an effect on the draft values at bow and stern. Interestingly, all codes predict a notable transient pitch angle in the beginning of flooding, whereas the measured pitch angle increases steadily.

Comparisons of water levels in the flooded compartments are presented in Fig. 13 at locations of four sensors. The sensor REL 6 is located in the intact side of a large U-shaped room. The extensive transient roll motion causes a smaller initial peak in the water level, and then the water level decreases back to zero until it starts to steadily increase due to cross-flooding after about 30 s. In general, this initial peak in water level is slightly over-estimated in simulations, and MSRC and UAK predict much larger peak and fail to capture the drying up of the sensor. KRISO estimates the peak well, but it occurs slightly faster than measured, which matches well with the simulation of the transient roll. UNITS simulation, with quasi-static ship motions, underestimates the water level peak and fails to capture the drying of the sensor.

Also measurement of cross-flooding on Deck 2 at sensor REL 14 contains a short initial water level peak that is not captured by any of the simulation codes, although CSSRC captures the start time of flooding at this sensor. The secondary flooding starts much earlier in simulations than in the experiment, which agrees with the roll response results. The secondary flooding between 30 and 60 s is well predicted by MARIN, NAPA and UAK. Both MSRC and UNITS estimate notably slower time for the whole sensor to be immersed, while KRISO predicts much too fast full immersion of the sensor. It should be noted that the sensor did not cover the whole deck height due to the sealings of the wires on the top, and this has been accounted in the plotted graphs of simulated water levels.

For sensor REL 28 on Deck 4, the codes predict correctly that the whole sensor is temporarily immersed during the transient roll motion. However, KRISO, MARIN, MSRC, NAPA and UAK simulations end with notably larger final water level than measured. Also the sensor REL 34 on Deck 6 is briefly completely immersed, and this is captured by KRISO, MARIN, MSRC and NAPA, although both MSRC and NAPA predict much longer period of immersion. MARIN has a proper timing and duration, but with fluctuations in the water level that were not recorded in the model tests.

As a summary, the following observations were made from the Case 1 results:

- CSSRC predicts the qualitative behavior of the ship well, but the smaller second peak of roll motion is not captured. Water levels are estimated well, although the code predicts lower maximum water level at REL 34.
- KRISO simulation captures the shape of the roll motion graph, including the second peak. However, the maximum transient roll angle is under-estimated, and the period of the transient roll motion is too short. Water level trends are captured, and the differences to the experimental results are likely due to the faster equalization of transient roll.
- MARIN simulation captures the maximum transient roll angle very well, and also the second peak is predicted. The roll decay seems to be slightly under-estimated. Water levels in the compartments are well predicted.

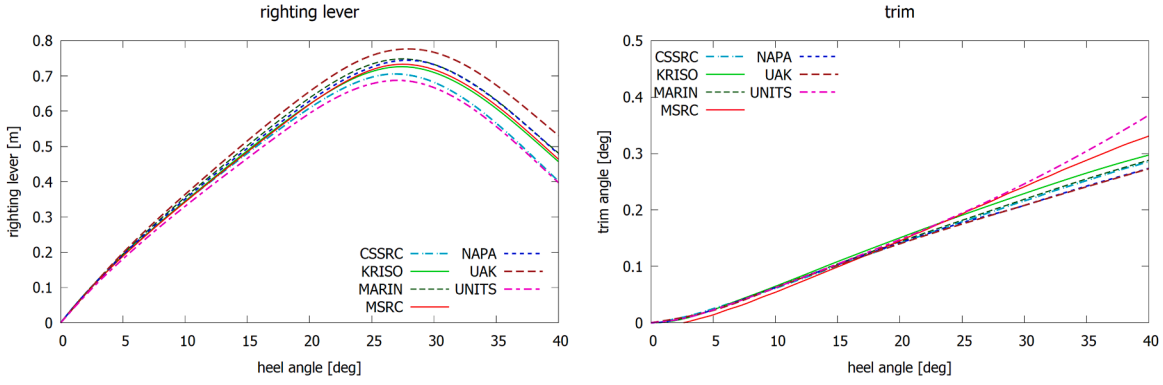

Fig. 9. Comparison of righting lever curves and related trim angles for the intact ship.

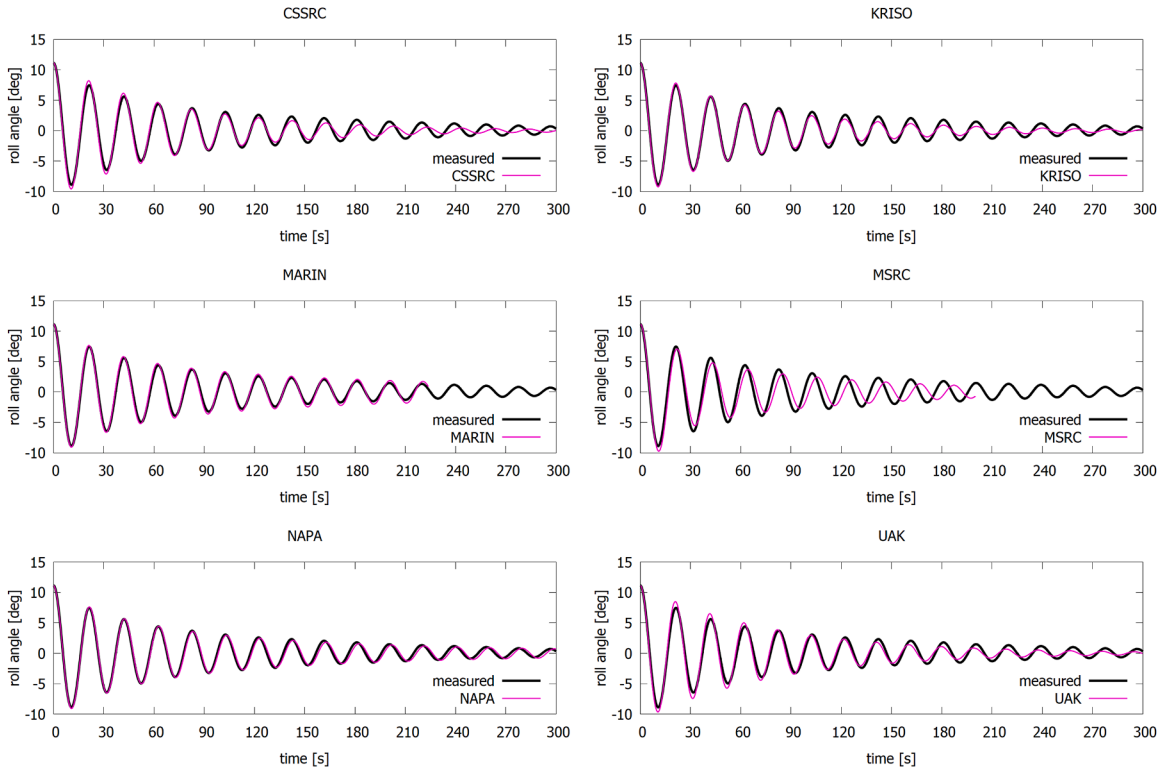

Fig. 10. Measured and simulated roll decay test for an intact ship.

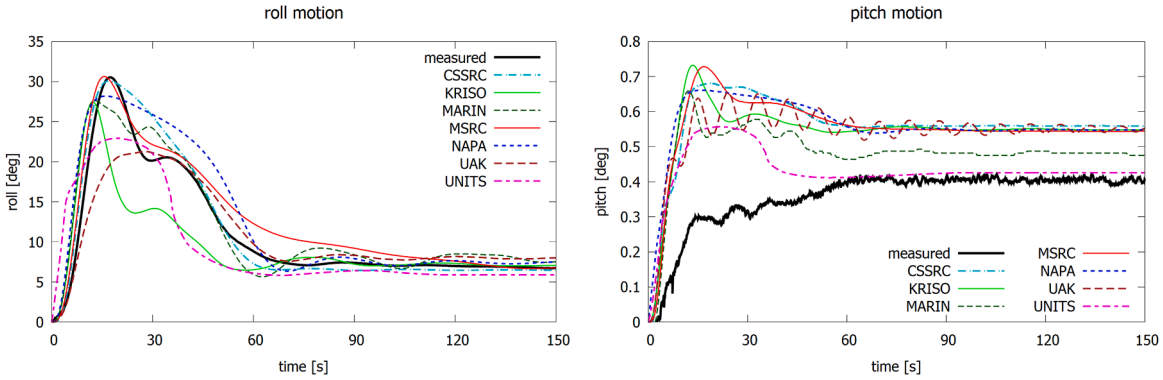

Fig. 11. Roll and pitch angles in the transient flooding benchmark Case 1.

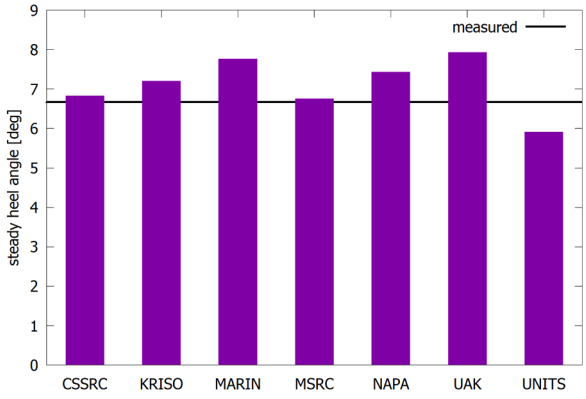

Fig. 12. Comparison of final steady heel angle in the Case 1

- MSRC captures the development of roll angle very well. However, the foremost breached compartment with cross-flooding had to be modelled as a single flooded room in order to avoid capsize in this case. In addition, there are notable differences in the water levels, especially in the cross-flooded compartment at REL 6.
- NAPA simulation is based on a simplified 1-DOF dynamic roll motion, yet the maximum transient roll angle is only slightly underestimated. However, the second peak is not captured, and the equalizing cross-flooding seems to be slightly slower than in the experiment. The water levels match rather well with the measurements.
- UAK simulation underestimates the transient roll angle, but after about 30 s the results match well with measurements, both for the roll angle and the water levels in the flooded compartments.
- UNITS simulation uses fully quasi-static ship motions, and therefore the transient roll angle is much smaller than measured, which also results in smaller water levels on the height decks, e.g. at REL 34. Otherwise, the flooding progression is captured well. Also UNITS

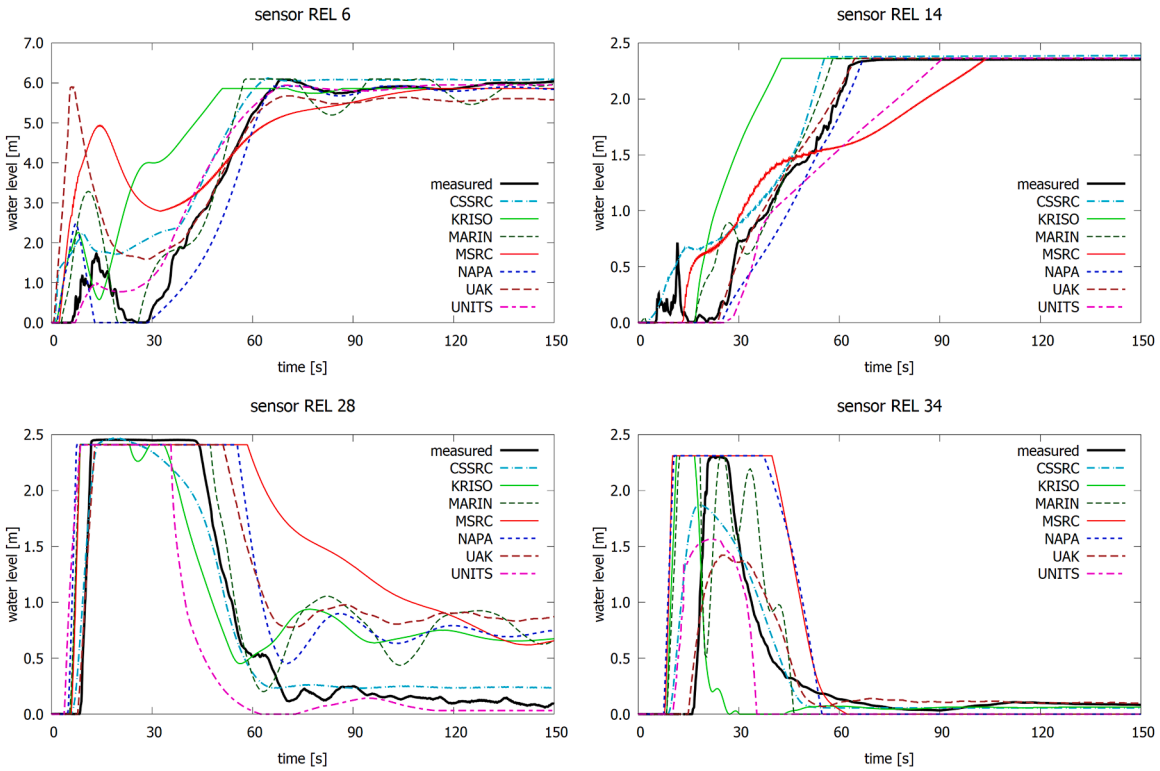

Fig. 13. Comparison of water levels in the flooded compartments in the test Case 1; sensor locations are shown in Fig. 5.

modelled the foremost breached compartment as a single room without cross-flooding.

6. Gradual progressive flooding in waves (Case 2)

6.1. Comparison of results with measured wave train

In the second benchmark test case the model is softly moored in irregular beam seas with the damage facing the waves, Fig. 14. JONSWAP wave spectrum ($\gamma = 7$ due to wavemaker limitation at high frequency and scale of the model) with significant wave height of 4.0 m and peak period of 8.0 s. The breach and intact conditions are the same as in the Case 1.

The maximum transient roll angle is about 30°, which is almost the same as in calm water in Case 1. Flooding is rapidly equalized, and roll angle reduces to less than 10°. Waves pump water to the bulkhead deck level (Deck 4), causing progressive flooding through the service corridor, and subsequent down-flooding to the undamaged compartment on Deck 3, as visualized in Fig. 15. This results in slow increase in the roll angle. There is further progressive flooding with larger roll angles when also Decks 5 and 6 are flooded through the breach opening, eventually causing a capsize at about 30 min (full scale).

The measured undisturbed wave history was provided as input to all participants. However, for KRISO the best matching simulation result out of 20 random realizations of the given sea state was used for comparison since the code does not support wave history input. The results for the roll angle are presented in Fig. 16.

CSSRC, MARIN and NAPA capture the transient roll motion rather well, while in the MSRC simulation the maximum transient roll is captured, but the decrease of transient roll is notably prolonged. KRISO underestimates the transient roll angle, but this could also be explained by the fact that a different wave realization was used.

KRISO and MSRC predict the time-to-capsize (TTC) rather accurately, although in the case of KRISO, the measured wave train was not used. MSRC also captures the temporary increase in the roll angle at around 15 min. In the simulation by KRISO the roll motion during progressive flooding is pronounced, compared to both measurement signal and other simulations. With CSSRC, MARIN and NAPA the TTC is notably shorter. NAPA simulation is based on a simple dynamic roll motion model, yet the transient roll motion is captured well, but flooding of the upper decks seems to be too fast, likely due to the applied quasi-static handling of heave motion, and consequently TTC is too short.

Time histories for water levels at four sensors are shown in Fig. 17.

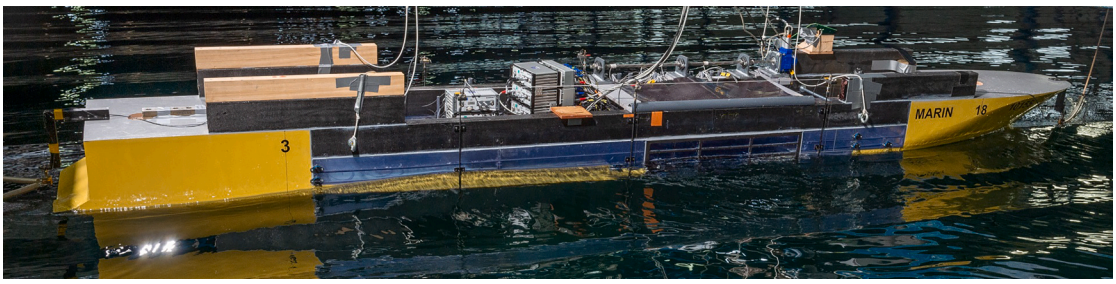

Fig. 14. Cruise ship model in irregular beam seas (courtesy of MARIN).

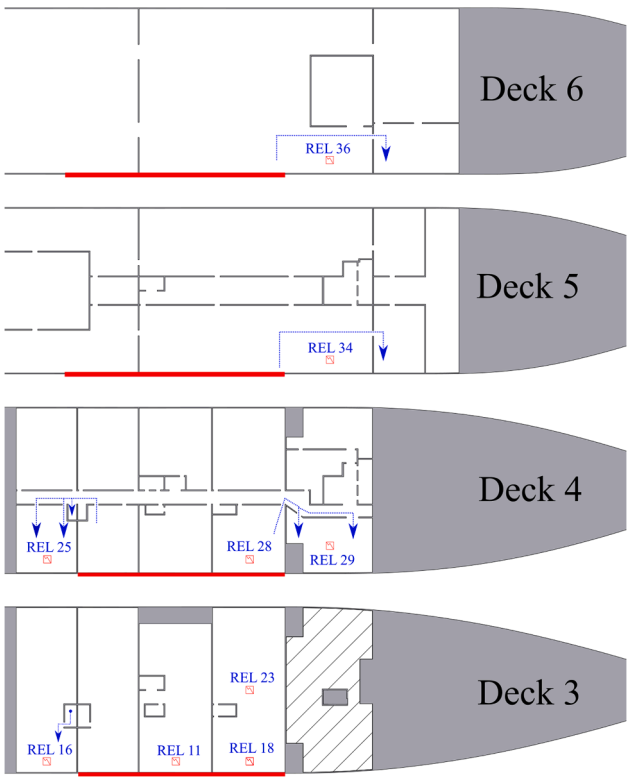

Fig. 15. Visualization of progressive flooding routes for the Case 2; in the aftmost compartment there is down-flooding from Deck 4 to Deck 3.

Although both MSRC and KRISO captured the TTC rather well, there are significant differences in the water levels. MSRC predicts well the water level peaks at REL 36 on Deck 6 that is temporarily flooded by high waves. However, MSRC predicts that the sensor REL 16 is fully immersed when the ship capsizes, whereas in the experiment the water level was significantly smaller. In the KRISO simulation the levels rise notable faster than measured, both at REL 16 and at REL 25. This indicates that although the capsize is properly captured, the actual flooding mechanism that leads to capsize is notably different.

6.2. Time-to-capsize

For a more comprehensive comparison between the different codes, all participants provided simulation results for 20 random realizations of the studied sea state. Results for the roll motion are shown in Fig. 18, together with measurements from three model tests using different wave trains. In two experiments the TTC is nearly identical, about 30 min in full scale, while in the third case the model capsized in about 20 min (in full scale).

In one of the CSSRC simulations the ship did not capsize within 40 min, while the other codes predict a capsize rate of 1.0. However, there is notable variation in TTC, as shown in Fig. 19. It is also noteworthy that all codes, except MARIN and NAPA, predict some rapid capsizes during transient flooding stage. MSRC predicts 50% likelihood for capsize within the first 10 min, whereas with other codes the clear majority of capsizes take place after the transient flooding stage. The number of experimental tests was limited to only 3, and therefore, a definite conclusion on the TTC cannot be drawn.

6.3. Drifting

In the experiments the model was kept positioned by a soft spring mooring system. The mooring lines were connected at the bow and stern of the vessel. The angle of the mooring lines was 45 degrees with the centerline. Line stiffness was reported by MARIN to be 241 kN/m and the pretension 6516 kN. The natural period of the mooring was about 5-times higher than the roll natural period, so that the soft mooring system does not affect the first order vessel motions. The mooring system prevents the model to drift away in the irregular wave. The second order drift loads will result in a slow oscillatory sway motions with respect to a mean sway offset due to the mean drift loads. The vessel position in the basin can only be predicted well if the mooring system and the second order drift loads are included in the numerical simulation set-up. Usually this is not the case since many codes neglect one or both affects (mooring loads and drift loads). The actual position of the ship in the wave spectrum realization will determine the relative wave velocity and the wave elevation at the damage opening and thus the ingress and egress of water.

A comparison of the drift is presented in Fig. 20. There is significant difference between KRISO and MSRC, both assuming free drift motion. Similar large variations in the simulated drift of the flooding ship in waves were found in the SAFEDOR benchmark study, Papanikolaou and Spanos (2008). Only MARIN modelled the mooring system, but the resulting sway motion in waves is notably smaller than measured. The fact that the MARIN simulation shows a lower amplitude of low frequent sway motions points to an under prediction of the sway draft load for the listed ship. This might be due to the fact that the drift loads from the upright ship are used since the potential seakeeping calculations were done for the intact loading condition only. In NAPA simulation the ship has a fixed transverse position.

It should be noted that most flooding simulation codes are intended for simulation of ship motions in full scale, and thus a feature to include the mooring line effects is normally not included. Even so, completely restraining the sway motion does not fully represent the model test

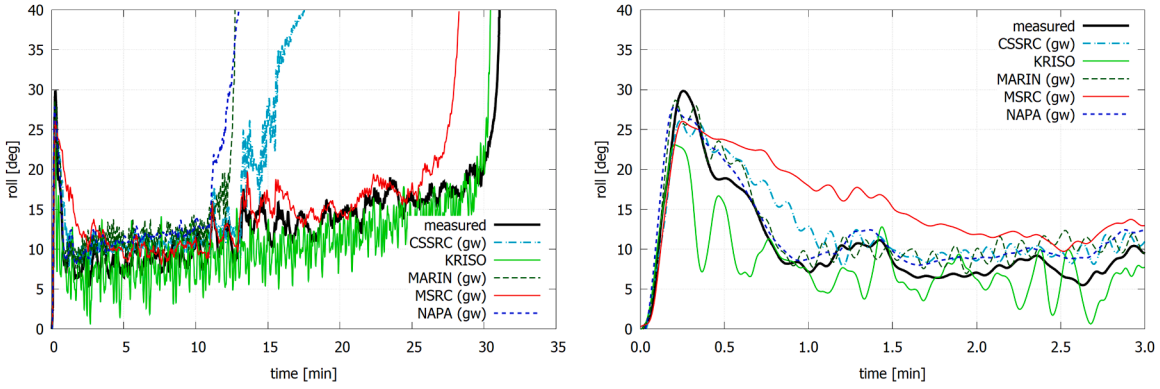

Fig. 16. Roll angle in the Case 2: codes marked with (gw) used the given wave train input, while for others the random realization of the given sea state with the best match has been selected; the graph on the right-hand side shows the details of transient roll motion.

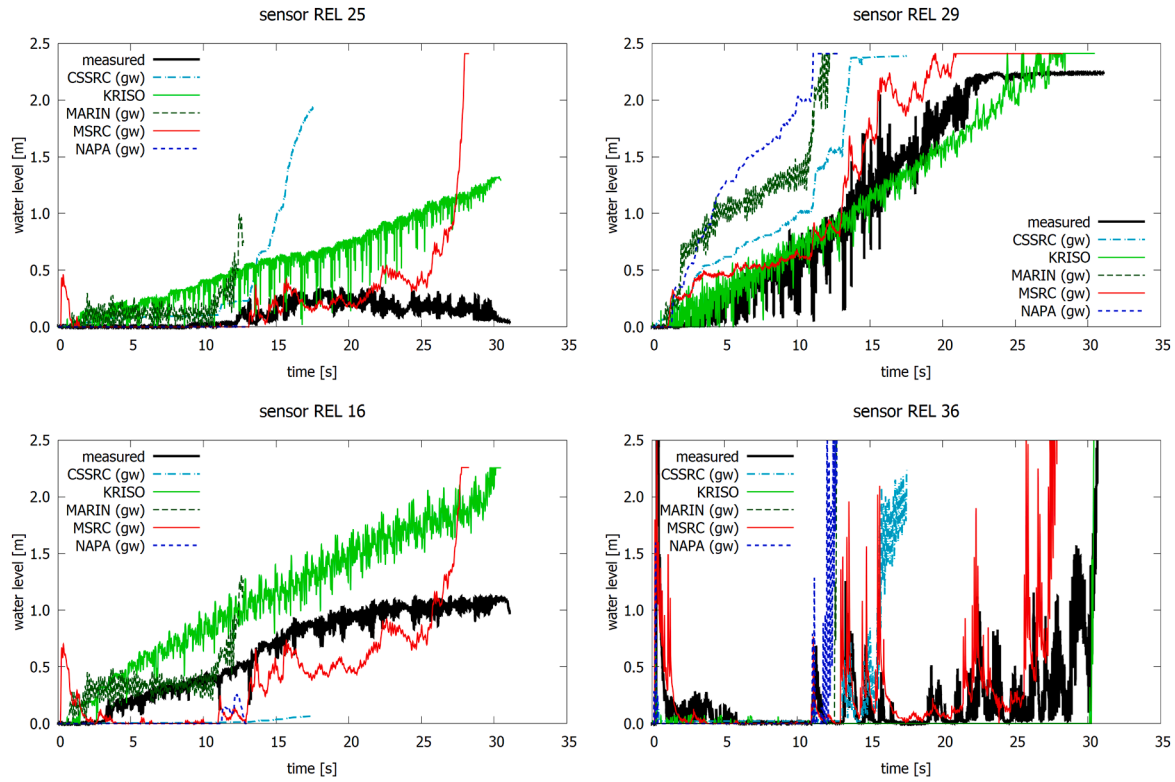

Fig. 17. Comparison of water levels in the flooded compartments in the test Case 2 (sensor locations are shown in Fig. 15); the curves are plotted up to the time when ship capsized (roll reached 40°).

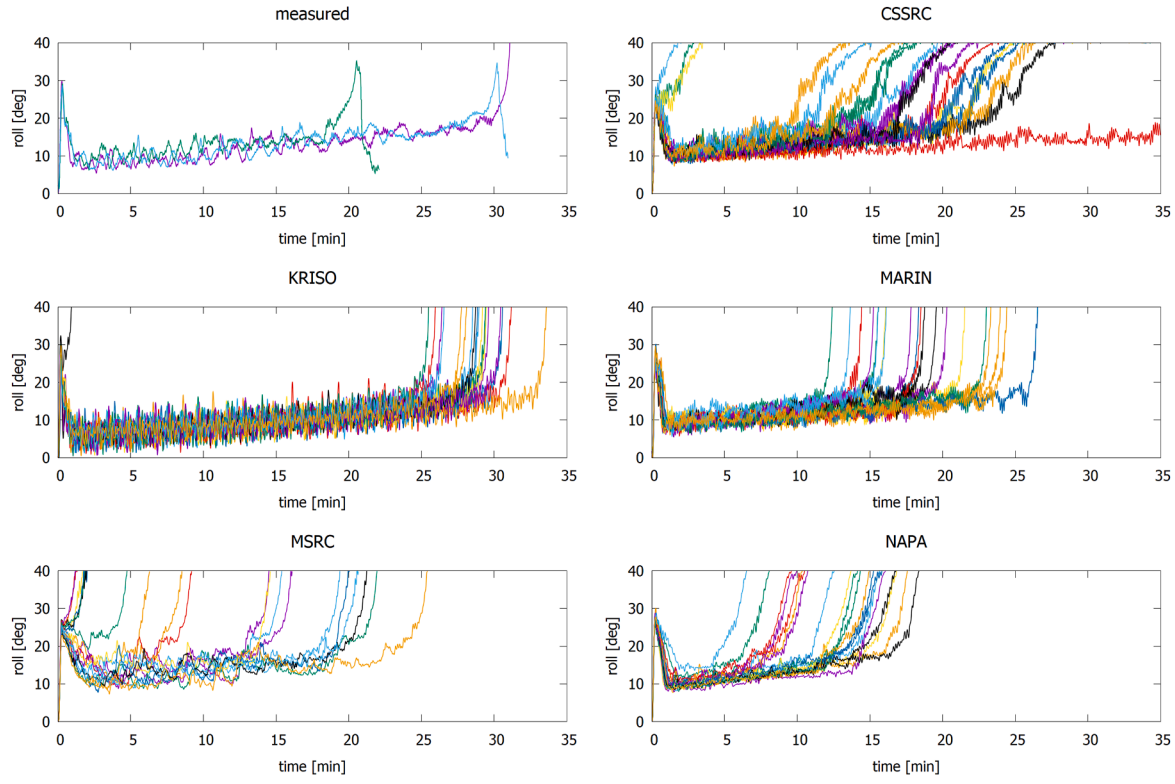

Fig. 18. Simulated development of roll angle in 20 realizations of the sea states and measured results in 3 realizations for Case 2.

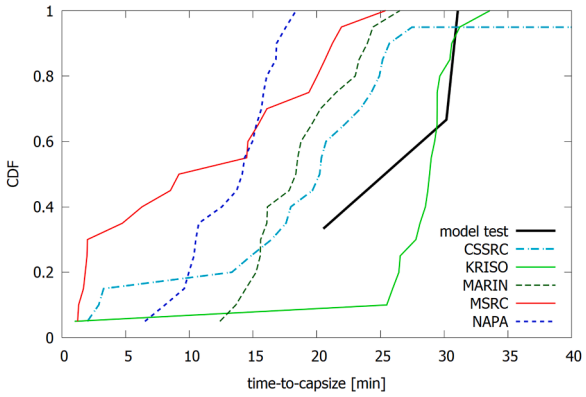

Fig. 19. Cumulative density functions (CDF) for time-to-capsize in the benchmark Case 2.

condition either.

7. Up-flooding in calm water (Case 3)

The third studied damage case is characterized by up-flooding through staircases. The same three compartments are damaged, but in this case the breach is vertically limited to the lowest two decks, as shown in Fig. 21. The routes of progressive flooding are visualized in Fig. 22. The model tests with the smaller breach size were conducted separately, after some participants had already conducted the calculations. Therefore, simulation results are presented for the original target intact GM of 2.36 m, whereas experimental results are shown separately for initial GM of 2.41 m and 2.29 m. The model test results show that the studied damage scenario is not very sensitive to the initial stability before flooding.

Results for the roll angle are shown in Fig. 23. CFD simulation by DNV slightly overestimates the maximum transient roll angle. Also the roll period is slightly longer than measured. It is believed that these differences are mainly caused by the slightly higher vertical center of gravity than with the other codes, as presented in Table 5. CSSRC, MARIN and MSRC predict this well, whereas KRISO and NAPA simulations slightly underestimate the peak. In the case of UAK, the maximum transient roll angle is notable smaller than measured, most likely since the large compartments in the bottom were not divided into parts. However, in general the subsequent roll motion is captured well by UAK. The fully quasi-static approach for ship motions by UNITS results in significantly smaller maximum roll angle and cannot capture the subsequent oscillations, but the final steady equilibrium angle is properly captured.

The final steady equilibrium is well predicted by CSSRC, MSRC and UNITS, whereas the other codes slightly overestimate it, Fig. 24. Likely reasons are small inaccuracies in the modelling of the flooded compartments and the slightly different KG values.

Like in Case 1, there is some variation in the final pitch angle, as shown in Fig. 25. However, the absolute differences are less than 0.1°. In general, the pitch angle is slightly overestimated, and only UNITS notably underestimates the final steady state pitch angle. It is worth noting that MARIN and UNITS simulations result in smaller final pitch angle than the other codes also for the Case 1, as shown in Fig. 11.

Comparisons of water levels at different sensors in the flooded rooms in Case 3 are shown in Fig. 26. The locations of the sensors are indicated in Fig. 22. The sensors REL 6 and REL 14 capture cross-flooding in the damaged compartments. In general, the development of water level is well predicted, although there is quite notable variation between the codes. Cross-flooding to the intact side (sensor REL 6) starts notably faster with the Bernoulli-based simulation codes than measured. But the CFD simulation by DNV captures this accurately, as well as the MARIN code that models flow inertia effects.

The sensors REL 11 and REL 18 capture the up-flooding to Deck 3 through the staircases. In the simulations, including also CFD, the up-flooding increases more rapidly compared to the measured water levels. The only exception is CSSRC, where the simulated water level at REL 18 matches well with the measurements. In UNITS simulation the

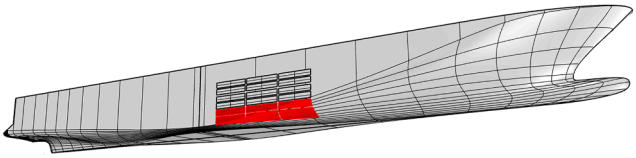

Fig. 21. Breach openings (red) for the up-flooding in the Case 3.

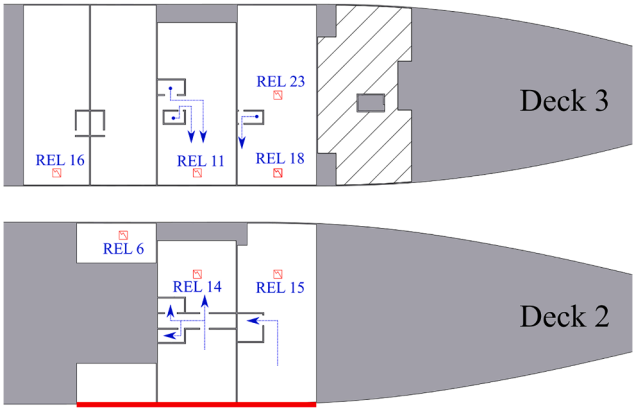

Fig. 22. Up-flooding routes from Deck 2 to Deck 3 in the Case 3.

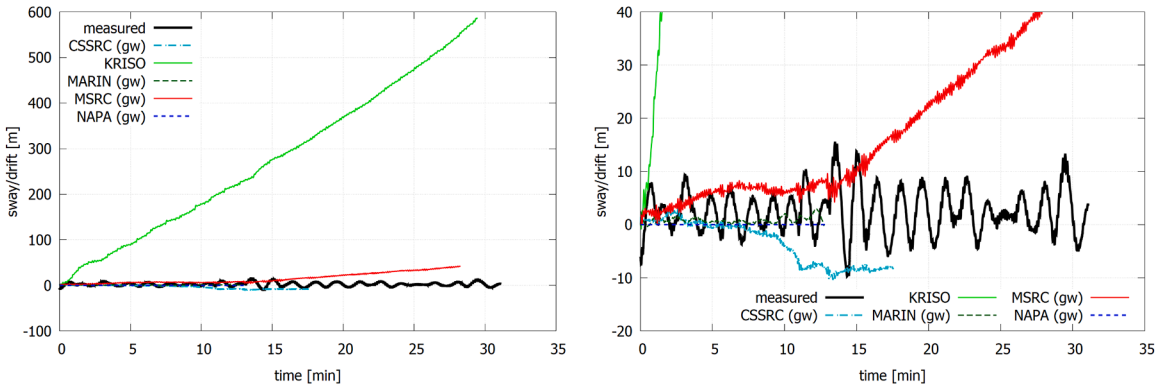

Fig. 20. Simulated drifting (i.e. sway motion) in the Case 2, the graph on the right shows the zoom to smaller values

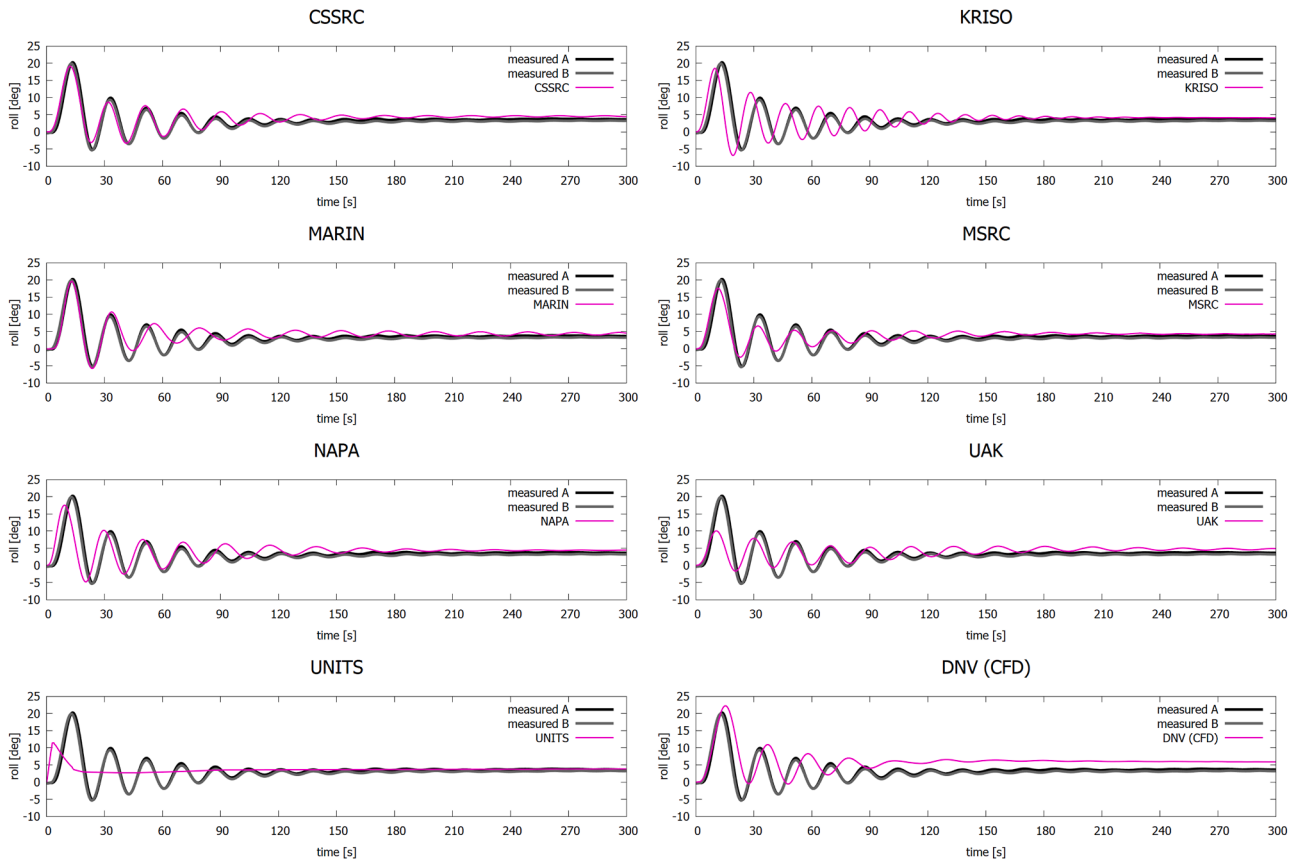

Fig. 23. Roll motion with different codes in the Case 3.

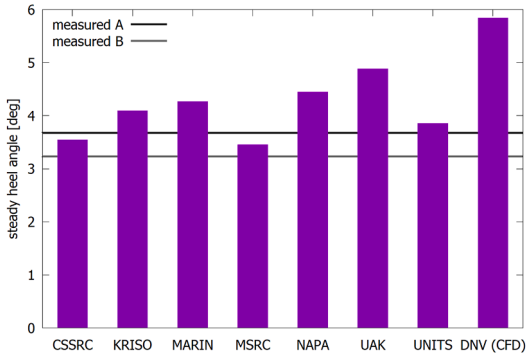

Fig. 24. Comparison of final steady heel angle with different codes in the Case 3

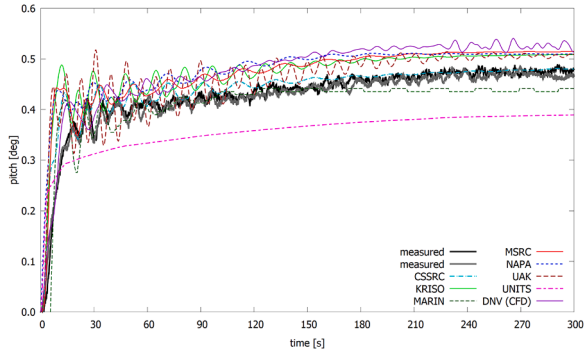

Fig. 25. Comparison of pitch motion with different codes in the Case 3.

water level at REL 11 is slower than measured, but at REL 18 somewhat faster. At both sensors the flow rate seems to slow down towards the equilibrium, a phenomenon that is also visible in the measurements. The CFD results with laminar flow model by DNV are in line with the Bernoulli-based methods. The up-flooding takes place through small vertical trunks (staircases and lifts), so the frictional flow losses on the trunk surfaces may be one explanation. Furthermore, the oscillations due to roll motion in the water levels at REL 11 and REL 18 are notably larger in the simulations than in the measurements.

The flooding condition at the maximum transient roll angle and at final condition are visualized in Fig. 27 from the CFD simulation results by DNV. At equilibrium, there is a small air pocket in the damaged side of the large U-shaped void in the aftmost compartment. Note that the air entrapment seen at the maximum transient roll in the complex aft compartment has disappeared in the final stage. These results indicate that air compression may have had some effect on the flooding progression in this damage case, but possible effects can be considered small.

8. Discussion

Flooding of a cruise ship with complex internal layout of the damaged compartments is a very complex process. This is challenging both in numerical simulation and in experimental tests in model scale. Unique tests were conducted in the EU Horizon 2020 project FLARE, that enabled an extensive benchmark study involving both transient and progressive flooding.

Compared to the latest ITTC benchmark study, van Walree and Papanikolaou (2007), some notable improvements are noted, both in the number of participants and in the quality of simulation results. Considering the results for progressive flooding in captive model tests in the first part of the FLARE benchmark, Ruponen et al. (2021), it is noted

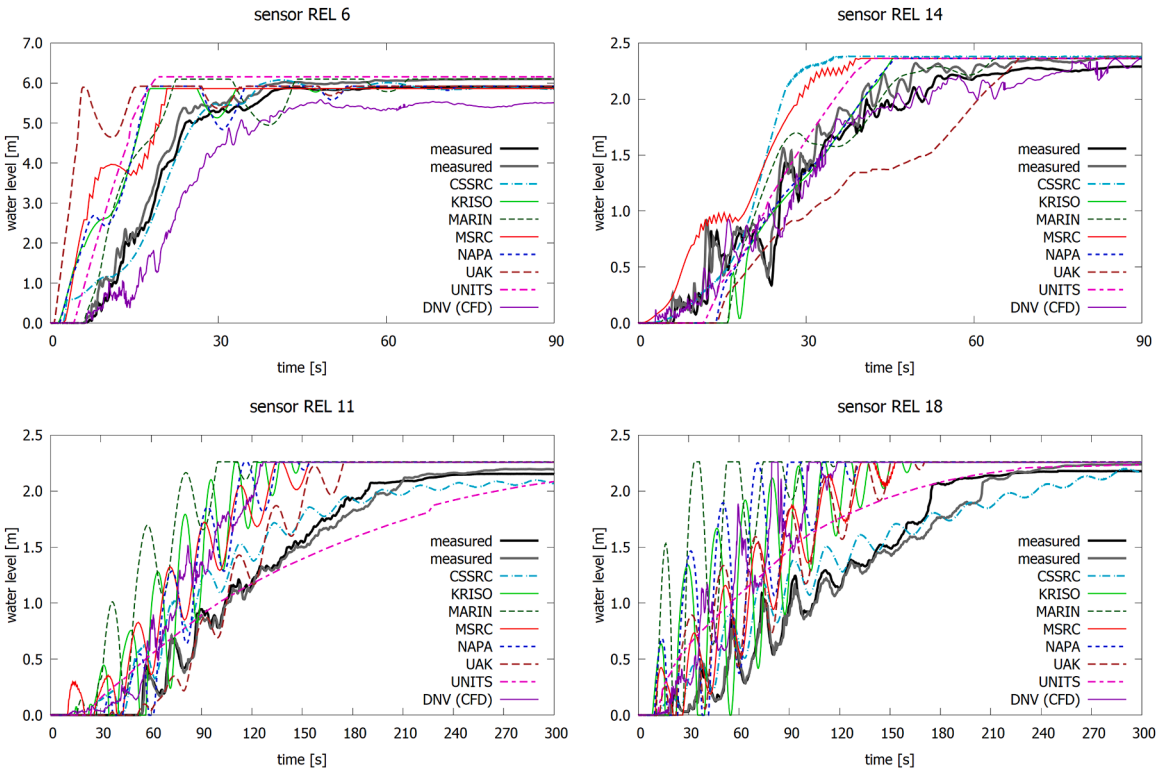

Fig. 26. Comparison of water levels in the flooded compartments in the test case 3 (sensor locations are shown in Fig. 22).

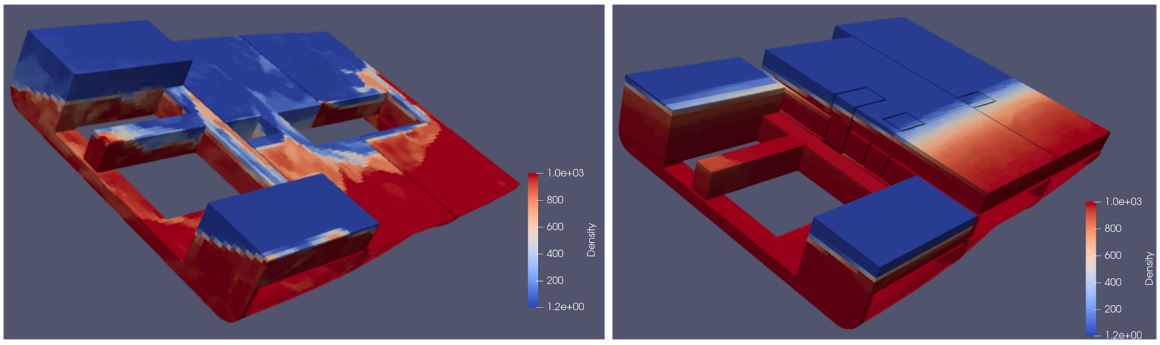

Fig. 27. Visualization of flooding progression inside the model in Case 3 from CFD results by DNV: maximum transient roll angle (left) and at final condition (right).

that all codes can capture the flooding progression rather realistically, but there is still notable deviation in the results. With a complex arrangement of flooded rooms of a cruise ship model, the differences are much larger, but the magnitude of transient roll angle can be captured well by most of the codes. Also the capsize in beam seas was properly predicted, but significant deviation was observed both in the time-to-capsize and in the distribution of floodwater at the time of capsize.

The main challenge with CFD tools is the required simulation time, making it currently unsuited for statistical evaluations with large numbers of simulations. The simulation codes that are based on a hydraulic model and Bernoulli's theorem are efficient, and the computations are typically notably faster than the simulated time. For CFD codes, the computation time is extensive, and in the Case 3, the computational time with CFD was almost 10 000 times longer than simulated time, even though model scale was used with assumption of laminar flow. Also the setup for the simulations is more laborious than with the simple and well-established Bernoulli-based codes. Although in general CFD can capture the internal flooding more realistically, instead of assuming that the water surfaces in the flooded rooms are either horizontal or inclined planes, in the present benchmark Case 3 the overall results are very similar with the other codes that are computationally much more efficient. Further studies on the benefits of CFD codes for detailed studies on flooding progression in complex arrangement of compartments should still be conducted, also considering turbulent flows and possible scale effects.

Although the hull form of the studied cruise ship design is very typical for modern large cruise ships, it was found out that it is not very suitable for benchmarking since the hydrostatic parameters are very sensitive to the modelling accuracy, especially at the selected intact draft. In future studies, a more conventional hull form should be adopted, along with somewhat simpler arrangement of the floodable compartments. Measured righting lever values for several heel angles should be given as input instead of specifying only the initial metacentric height. In addition, the effects of the mooring lines should be studied. Experiments with a freely drifting mode could be used, as instructed in ITTC (2017), which is a more realistic condition for a damaged ship in waves. On the other hand, then the drift loads should be modelled in the

codes in order to get to the same timing of the model in waves. Also a smaller ship could be used, allowing a larger scale that would reduce the possible scale effects in the results.

9. Conclusions

Time-domain simulation of flooding and damaged ship motion is becoming a viable tool for survivability assessment for design of safer passenger ships. Consequently, validation and benchmarking of the applied simulation codes is essential. For this purpose, dedicated model tests have been conducted in the project FLARE, enabling an extensive benchmark study. The vast amount of internal wave probes in the model to measure the water levels throughout the flooded compartments was an essential part in the study.

The results show that time-domain simulation tools can capture the maximum transient roll angle for a passenger ship with an extensive breach and dense internal subdivision in the damaged compartments. On the other hand, notable differences were observed in the distribution of water inside the compartments during the flooding process. In calm water the differences were smaller, but in beam seas also the capsize mechanism was considered to be different between the codes. This indicates that further research and development of the simulation codes are still needed, especially regarding the effects of waves on the flooding process. On the other hand, the qualitative results of the benchmark study are rather promising, and the status of the flooding simulation tools have considerably improved compared to the last ITTC benchmark study, where a rather simple progressive flooding scenario in calm water was not properly captured by most of the codes. Based on the new results, the Bernoulli-based simulation codes, with proper modelling of roll dynamics and irregular waves, are considered suitable for survivability assessments of ships with dense internal non-watertight subdivision, such as cruise ships, with a focus on the probability of capsizing instead of the details of progressive flooding and accurate time-to-flood.

CRediT authorship contribution statement

Pekka Ruponen: Conceptualization, Methodology, Writing – original draft, Visualization, Writing – review & editing. **Rinnert van Basten Batenburg:** Conceptualization, Data curation, Investigation, Writing – review & editing. **Riaan van't Veer:** Conceptualization, Investigation, Writing – review & editing. **Luca Braidotti:** Investigation, Writing – review & editing. **Shuxia Bu:** Investigation, Writing – review & editing. **Hendrik Dankowski:** Investigation, Writing – review & editing. **Gyeong Joong Lee:** Investigation, Writing – review & editing. **Francesco Mauro:** Investigation, Writing – review & editing. **Eivind Ruth:** Investigation, Writing – review & editing. **Markus Tompuri:** Investigation, Writing – review & editing.

Declaration of Competing Interest

The authors declare that they have no known competing financial interests or personal relationships that could have appeared to influence the work reported in this paper.

Data Availability

Data will be made available on request.

Acknowledgments

The presented research has received funding from European Union project FLooding Accident REsponse (FLARE) number 814753, under H2020 programme. The authors express their gratitude for this support. Chantiers d'Atlantique is thanked for providing the ship design. The views set out in this paper are those of the authors and do not necessarily reflect the views of their respective organizations.

References

Atzampos, G., Vassalos, D., Cichowicz, J., Paterson, D., Boulougouris, E., 2019. eSAFE - cruise ship survivability in waves. In: Proceedings of the 17th International Ship Stability Workshop, 10-12 June 2019. Helsinki, Finland, pp. 265–274.

Bačkalov, I., Bulian, G., Cichowicz, J., Eliopoulou, E., Konovessis, D., Leguen, J.F., Rosén, A., Themelis, N., 2016. Ship stability, dynamics and safety: status and perspectives from a review of recent STAB conferences and ISSW events. Ocean Eng. 116, 312–349. https://doi.org/10.1016/j.oceaneng.2016.02.016.

Braidotti, L., Mauro, F., 2019. A new calculation technique for onboard progressive flooding simulation. Ship Technol. Res. 66 (3), 150–162. https://doi.org/10.1080/09377255.2018.1558564.

Braidotti, L., Mauro, F., 2020. A fast algorithm for onboard progressive flooding simulation. J. Mar. Sci. Eng. 8 (5), 369. https://doi.org/10.3390/jmse8050369.

Braidotti, L., Dega, G., Bertagna, S., Bucci, V., Marino, A., 2021. A comparison of different linearized formulations for progressive flooding simulations in full-scale. Procedia Comput. Sci. 180, 219–228. https://doi.org/10.1016/j.procs.2021.01.159.

Braidotti, L., Prpić-Oršić, J., Valčić, M., 2022. Free-outflow modelling in the linearised progressive flooding simulation methodology. In: Proceedings of the 15th International Symposium on Practical Design of Ships and Other Floating Structures PRADS 2022. Dubrovnik, Croatia, p. 2022.

Bu, S., Gu, M., Lu, J., 2018. Prediction of damaged ship motions in waves in time domain. Sh. Build. China 59 (2), 80–89 in Chinese.

Bu, S., Qi, J., Gu, M., 2020. Study on capsizing characteristics and influencing factors of damaged ship in regular waves. Sh. Build. China 61 (4), 60–69, 2020in Chinese.

Caldas, A., Zegos, C., Skoupas, S., Jenkins, J., 2018. Ship survivability study using high fidelity CFD. Technology and Science for the Ships of the Future. IOS Press, pp. 141–148.

Cho, S., Sung, H., Nam, B., Hong, S., Kim, K., 2009. Experimental study on flooding of a cruiser in waves. In: Proceedings of the 10th International Conference on Stability of Ships and Ocean Vehicles STAB2009. St. Petersburg, Russia, pp. 747–753.

Dankowski, H., 2013. A Fast and Explicit Method for the Simulation of Flooding and Sinkage Scenarios on Ships. Hamburg University of Technology. PhD Thesis at. https://tore.tuhh.de/handle/11420/1127.

Dankowski, H., Krüger, S., 2015. Dynamic Extension of a numerical flooding simulation in the time-domain. In: Proceedings of the 12th International Conference on the Stability of Ships and Ocean Vehicles STAB2015. Glasgow, UK.

FLARE, 2018-2022. FLARE FLooding Accident Response, EU Funded Research Project, Horizon 2020, Contract No.: 814753, Website: http://www.flare-project.eu.

Gao, Z., Vassalos, D., Gao, Q., 2010. Numerical simulation of water flooding into a damaged vessel's compartment by the volume of fluid method. Ocean Eng. 37 (16), 1428–1442. https://doi.org/10.1016/j.oceaneng.2010.07.010.

HARDER, 2000-2003. HARDER harmonization of rules and design rational, EU Funded Research Project FP5. https://cordis.europa.eu/project/id/G3RD-CT-1999-00028.

Idel'chik, I.E., 1960. Handbook of Hydraulic Resistance. U.S. Atomic Energy Commission, Washington D.C (translated from Russian), Published for the.

Ikeda, Y., Shimoda, S., Takeuchi, Y., 2003. Experimental studies on transient motion and time to sink of a damaged large passenger ship. In: Proceedings of the 8th International Conference on Stability of Ships and Ocean Vehicles STAB2003. Madrid, Spain, pp. 243–252.

Ikeda, Y., Ishida, S., Katayama, T., Takeuchi, Y., 2011. Experimental and numerical studies on roll motion of a damaged large passenger ship in intermediate stages of flooding. Contemporary Ideas on Ship Stability and Capsizing in Waves. In: Almeida Santos Neves, M., Belenky, V., de Kat, J., Spyrou, K., Umeda, N. (Eds.), In: Fluid Mechanics and Its Applications, 97. Springer, Dordrecht, pp. 633–641. https://doi.org/10.1007/978-94-007-1482-3_36.

Italy 2004a. Development of revised SOLAS Chapter II-1 Parts A, B and B-1: Damage stability probabilistic approach SAFENVSHIP extension research activities, IMO SLF 47/3/5, 11 June 2004.

Italy 2004b. Large Passenger Ship Safety: Damage stability model tank test for a large passenger ship, IMO SLF 47/8/2, 9 July 2004.

ITTC 2017. Model tests on damage stability in waves, ITTC quality system manual: recommended procedures and guidelines, 7.5–02-07–04.2, Rev. 03. https://www.ittc.info/media/8145/75-02-07-042.pdf.

Jasionowski, A., 2001. An Integrated Approach to Damage ship Survivability Assessment. University of Strathclyde. PhD thesis. http://oleg.lib.strath.ac.uk/R/?func=dbin-jump-full&object_id=20411.

Katayama, T., Ikeda, Y., 2005. An Experimental study of fundamental characteristics of inflow velocity from damaged opening. In: Proceedings of the 8th International Ship Stability Workshop, ISSW2005. Istanbul, Turkey, 6-7 October 2005.

Lee, G.J., 2015a. Flow model for flooding simulation of a damaged ship. In: Proceedings of the 12th International Conference on the Stability of Ships and Ocean Vehicles (STAB 2015). Glasgow, UK, pp. 931–951, 14-19 June 2015.

Lee, G.J., 2015b. Dynamic orifice flow model and compartment models for flooding simulation of a damaged ship. Ocean Eng. 109, 635–653. https://doi.org/10.1016/j.oceaneng.2015.09.051.

Letizia, L., 1996. Damage Survivability of Passenger Ships in a Seaway. University of Strathclyde. PhD thesis. https://stax.strath.ac.uk/concern/theses/pn89d666g.

Lorkowski, O., Dankowski, H., Kluwe, F., 2014. An experimental study on progressive and dynamic damage stability scenarios. In: Proceedings of the ASME 2014 33rd International Conference on Ocean, Offshore and Arctic Engineering. American Society of Mechanical Engineers Digital Collection. https://doi.org/10.1115/OMAE2014-23388.

Macfarlane, G.J., Renilson, M.R., Turner, T., 2010. The transient effects of flood water on a warship in calm water immediately following damage. Trans. R. Inst. Nav. Archit. A Int. J. Marit. Eng. 152 (4), A209–A224.

Manderbacka, T., Themelis, N., Bačkalov, I., Boulougouris, E., Eliopoulou, E., Hashimoto, H., Konovessis, D., Leguen, J.F., Míguez González, M., Rodríguez, C.A., Rosén, A., Ruponen, P., Shigunov, V., Schreuder, M., Terada, D., 2019. An overview of the current research on stability of ships and ocean vehicles: the STAB2018 perspective. Ocean Eng. 186, 1–16. https://doi.org/10.1016/j.oceaneng.2019.05.072. Article 106090.

Mauro, F., Vassalos, D., Paterson, D., Boulougouris, E., 2022. Exploring smart methodologies for critical flooding scenarios detection in the damage stability assessment of passenger ships. Ocean Eng. 262, 112289 https://doi.org/10.1016/j.oceaneng.2022.112289.

Papanikolaou, A., Zaraphonitis, G., Spanos, D., Boulougouris, E., Eliopoulou, E., 2000. Investigation into the capsizing of damaged Ro-Ro passenger ships in waves. In: Proceedings of the 7th International Conference on Stability of Ships and Ocean Vehicles STAB 2000. Launceston, Tasmania, Australia, pp. 351–362.

Papanikolaou, A.D., 2007. Review of damage stability of ships – recent developments and trends. In: Proceedings of the 10th International Symposium on Practical Design of Ships and Other Floating Structures (PRADS). Houston, USA. October 2007.

Papanikolaou, A., Spanos, D. 2001. Benchmark study on the capsizing of a damaged Ro-Ro passenger ship in waves – Final Report.

Papanikolaou, A., Spanos, D. 2005. The 24th ITTC benchmark study on numerical prediction of damage ship stability in waves – Final Report.

Papanikolaou, A., Spanos, D. 2008. Benchmark study on numerical codes for the prediction of damage ship stability in waves, ISSW2008.

Ruponen, P., 2007. Progressive Flooding of a Damaged Passenger Ship, Dissertation for the degree of Doctor of Science in Technology. Helsinki University of Technology. TKK Dissertations 94, 124 p. https://aaltodoc.aalto.fi/handle/123456789/2931.

Ruponen, P., Sundell, T., Larmela, M., 2007. Validation of a simulation method for progressive flooding. Int. Shipbuild. Prog. 54, 305–321.

Ruponen, P., Kurvinen, P., Saisto, I., Harras, J., 2010. Experimental and Numerical Study on Progressive Flooding in Full-Scale. Trans. R. Inst. Nav. Archit. Int. J. Marit. Eng. 152, A-197-207.

Ruponen, P., Queutey, P., Kraskowski, M., Jalonen, R., Guilmineau, E., 2012. On the calculation of cross-flooding time. Ocean Eng. 40, 27–39. https://doi.org/10.1016/j.oceaneng.2011.12.008.

Ruponen, P., 2014. Adaptive time step in simulation of progressive flooding. Ocean Eng. 78, 35–44. https://doi.org/10.1016/j.oceaneng.2013.12.014.

Ruponen, P., Lindroth, D., Routi, A.L., Aartovaara, M., 2019. Simulation-based analysis method for damage survivability of passenger ships. Ship Technol. Res. 66 (3), 180–192. https://doi.org/10.1080/09377255.2019.1598629.

Ruponen, P., van Basten Batenburg, R., Bandringa, H., Braidotti, L., Bu, S., Dankowski, H., Lee, G.J., Mauro, F., Murphy, A., Rosano, G., Ruth, E., Tompuri, M., Valanto, P., van't Veer, R, 2021. Benchmark Study on Simulation of Flooding Progression. In: Proceedings of the 1st International Conference on the Stability and Safety of Ships and Ocean Vehicles. Glasgow, Scotland, UK, 7-11 June 2021.

Ruponen, P., Valanto, P., Acanfora, M., Dankowski, H., Lee, G.J., Mauro, F., Murphy, A., Rosano, G., van't Veer, R., 2022. Results of an international benchmark study on numerical simulation of flooding and motions of a damaged ropax ship. Appl. Ocean Res. 123 https://doi.org/10.1016/j.apor.2022.103153. Article 103153.

Ruth, E., Olufsen, O., Rognebakke, O., 2019. CFD in damage stability. In: Proceedings of the 17th International Ship Stability Workshop. Helsinki, Finland, pp. 259–263, 10-12 June 2019.

SAFEDOR 2005-2009. SAFEDOR (design, operation and regulation for safety), EU Funded Research Project FP6. https://cordis.europa.eu/project/id/516278.

SAFENVSHIP 2002-2006. SAFENVSHIP SAFe and ENVironmental Friendly Passenger SHIPs, R&D project jointly funded under the EUREKA scheme, by a number of companies and by several EU member states.

Santos, T.A., Winkle, I.E., Guedes Soares, C., 2002. Time domain modelling of the transient asymmetric flooding of Ro-Ro ships. Ocean Eng. 29 (6), 667–688. https://doi.org/10.1016/S0029-8018(01)00037-3.

Schindler, M., 2000. Damage stability tests with models of ro-ro ferries – a cost effective method for upgrading and designing ro-ro ferries. Contemporary Ideas on Ship Stability. Elsevier, pp. 213–224.

Spanos, D., Papanikolaou, A., 2014. On the time for the abandonment of flooded passenger ships due to collision damages. J. Mar. Sci. Technol. 19, 327–337. https://dx.doi.org/10.1007/s00773-013-0251-0.

van't Veer, R., 2001. Model Test Results PRR02, Report (3-31-D-2001-07-0), European Commission research project on Harmonization of Rules and Design Rationale HARDER.

van't Veer, R., de Kat, J., Cojeen, P., 2004. Large Passenger Ship Safety: Time-to-Flood Simulations. Mar. Technol. 41 (2), 82–88.

van't Veer, R., van den Berg, J., Boonstra, S., van Basten-Batenburg, R., Bandringa, H., 2021. A steady and unsteady internal flooding model utilizing a network and graph solver. In: Proceedings of the 1st International Conference on the Stability and Safety of Ships and Ocean Vehicles. Glasgow, Scotland, UK, 7-11 June 2021.

Vassalos, D., 2016. Damage survivability of cruise ships - Evidence and conjecture. Ocean Eng. 121, 89–97. https://doi.org/10.1016/j.oceaneng.2016.04.033.

van Walree, F., Papanikolaou, A., 2007. Benchmark study of numerical codes for the prediction of time to flood of ships: Phase I. In: Proceedings of the 9th International Ship Stability Workshop ISSW2007. Hamburg, Germany.

Ypma, E.L., Turner, T., 2019. An approach to the validation of ship flooding simulation models. Contemporary Ideas on Ship Stability, pp. 637–675. https://doi.org/10.1007/978-3-030-00516-0_38.